Theoretical optoelectronic analysis of $MgIn_2S_4$ and $CdIn_2S_4$ thiospinels: Effect of transition-metal substitution in intermediate-band formation

I. Aguilera, P. Palacios, K. Sánchez, and P. Wahnón
Instituto de Energía Solar and Departamento Tecnologías Especiales, ETSI Telecomunicación, UPM, Ciudad Universitaria, Madrid 28040, Spain

We analyzed and compared two families of intermediate-band materials derived from indium thiospinels: $MgIn_2S_4$, having an inverse spinel structure, and $CdIn_2S_4$, a direct spinel. First-principles studies of the electronic structures of these two parent semiconductors were carried out to understand the nature of their band gaps. Optical properties were also analyzed and we found good agreement with experiments. As derivatives of these semiconductors, alloys where transition metals (M=Ti and V) substitute for In atoms at octahedral sites are presented as a class of intermediate-band materials. First, the effect of the substitution on structural parameters is assessed. Then, electronic structures are determined for $Mg_2MIn_3S_8$ and $Cd_2MIn_3S_8$ to show that the t_{2g} d states of the transition metal form a partially filled localized band within the band gap of the host semiconductor. The suitability of these compounds as photovoltaic high-efficiency absorbers is discussed. An increase in absorption is assessed by studying the contribution of the transition-metal band toward their optical properties, in the range of higher solar emission, and comparing them with those of the host semiconductors. An analysis of transmittance spectra is carried out to predict the range of optimum thicknesses for samples of this type of thin film absorber. We compare, by means of structural, electronic, and optical behavior, Ti and V as substituents, to evaluate the resulting alloys for potential photovoltaic applications.

PACS number(s): 78.20.Ci, 71.20.Be, 71.15.Mb

I. INTRODUCTION

The great effort to achieve more efficient lower-cost photovoltaic solar cells has led to the combination of the intermediate-band (IB) concept and thin-film technology. A compromise between the two could be the answer to the present high-efficiency low-cost challenge.

The intermediate-band concept was proposed as a solution to the efficiency problem. This is because a partially filled narrow band that is isolated from the valence and conduction bands of a host semiconductor would allow the absorption of subband-gap energy photons. For a solar cell, this would result, in the creation of additional electron-hole pairs and, in principle, in an increase in photocurrent without a decrease in open-circuit voltage. A cell based on such an approach could reach theoretical efficiencies up to 63.2%.[1]

However, a greater absorption of photons does not necessarily mean a greater photocurrent, as very localized levels could favor nonradiative recombination. Therefore, in order to be efficient, an intermediate band has to fulfill some requirements. It has to have a small dispersion and must not be a discrete level; however, at the same time, it has to be narrow enough to be well isolated from the valence and conduction bands, to avoid thermalization to the IB. It also has to be partially filled, to allow comparable rates for the two possible absorption processes involving the IB. In addition, materials presented here have advantage of spin polarization, as the spin selection rules for electronic transitions can improve the enhancement in lifetimes for the generated electron-hole pairs.[2]

The first materials proposed to combine the intermediate-band concept with thin-film technology (intended to reduce the costs) were derivatives of chalcopyrites. Studies of intermediate-band materials based on $CuGaS_2$ have already been presented,[3] showing a potential suitability for enhanced photovoltaic applications. In these materials, Ga atoms were replaced by Ti or Cr (at tetrahedral sites). It is well known[4] that the octahedral environment is thermodynamically more stable for these transition metals. This is because there is a preference to be surrounded by six atoms, rather than by four. This necessitates a deeper study of the intermediate-band formation by transition metals at octahedral sites, thus motivating the present study of thiospinel derivatives.

Very recently, we presented the *ab initio* optical properties of the spinel semiconductor In_2S_3, where octahedral In atoms were replaced by V or Ti.[4] V-substituted In_2S_3 was synthesized later, due to our promising predictions. This was the first time that a partially filled intermediate-band material, absorbing across the full solar spectrum range, was synthesized. Its optical properties were later measured, showing very good agreement with our theoretical results.[5] Thus, the prediction capabilities of our methodology were confirmed.

The two thiospinel host semiconductors presented here were chosen as potential candidates for intermediate-band formation because their band gaps lie in the region of optimum gaps for the implementation of an IB material.[1] $MgIn_2S_4$ has a band gap ranging from 2.1 to 2.28 eV,[6,7] but vacancies of Mg can significantly affect this value. In addition, Ref. 8 assumes it is a direct gap, but this is not clear.[6,7,9] Therefore, further study is needed. In the case of $CdIn_2S_4$, the direct band gap shows a wide range of values in the literature: it varies from 2.35 to 2.62 eV. Yet, there is also some controversy as to whether this gap is direct[8,10] or indirect.[11–13]

Both thiospinels are photoactive in the visible region of the spectrum and are currently used for optoelectronic applications as photoconductors. They crystallize in the cubic spinel structure, where Mg or Cd atoms occupy tetrahedral

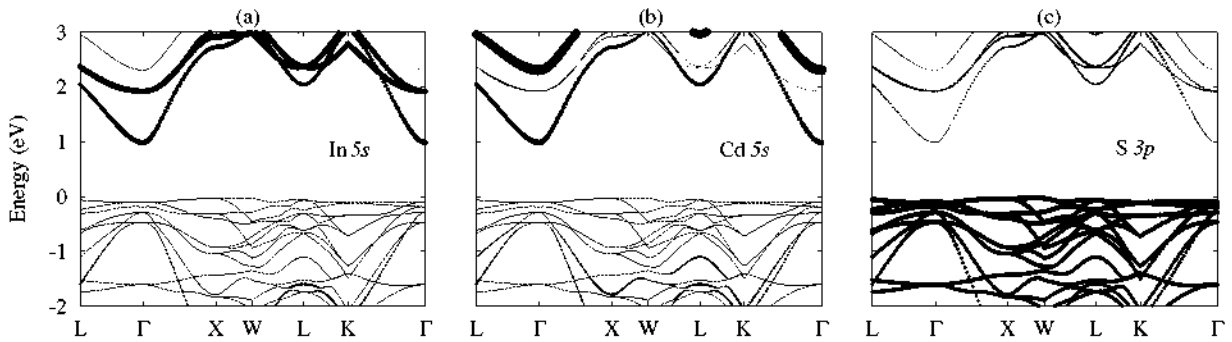

FIG. 1. (Color online) Projection of the band diagram of $CdIn_2S_4$, where the circles size is proportional to the orbital projections of the (a) In 5*s*, (b) Cd 5*s*, and (c) S 3*p* states divided by the number of atoms of each species. The contribution of other orbitals is comparatively negligible in this energy range. As a guide to the eye, the band diagram containing all the states is represented as a thin dashed line.

sites, whereas In has octahedral coordination. However, for the two compounds presented here, the structures found in nature have some degree of inversion. In other words, some cations interchange their positions in the cell structure. Attempts to determine this degree of inversion theoretically have failed.[14] This may be related to the fact that this parameter is very dependent on temperature[15] and most *ab initio* calculations are limited to zero temperature.

The main purpose of the present work is to compare, in detail, the effect of the structural degree of inversion in spinel compounds on the formation of the intermediate band, by studying a direct and an inverse structure and comparing them. The effect of two promising transition-metal substituents (Ti and V) on the formation and characteristics of the intermediate band will be studied, as well as the enhancement of optical absorption properties in the resulting compounds. In Sec. II, we describe the approaches followed. Section III shows the results of structural, electronic, and optical properties. Finally, Sec. IV summarizes our conclusions.

II. METHOD

In this work, the electronic ground state of each material was calculated with spin-polarized density functional theory (DFT) in the generalized gradient approximation (GGA) with the Perdew-Wang 1991 functional,[16] using the plane-wave code VASP.[17] Projector augmented wave pseudopotentials[18,19] were used to describe electron-ion interactions. The valence configurations used in this work were $3s^2$ for Mg; $5s^24d^{10}$ for Cd; $5s^25p^1$ for In; $3s^23p^4$ for S; $4s^13d^5$ for Ti; and $4s^13d^4$ for V.

In all cases, the cells and ions were fully relaxed with a tolerance for atomic forces of 0.01 eV/Å.

Concerning the optical properties, we obtained the imaginary part of the dielectric tensor as a sum over independent Kohn-Sham transitions, as given by Fermi's golden rule. Further details of this method are described in Ref. 20 and implemented in the OPTICS code.[21] This approach is an independent-particle approach, such that it neglects electron-electron and electron-hole interactions. The local-field effects (i.e., the off-diagonal elements of the dielectric matrix) are also neglected. However, this method has been tested successfully on an intermediate-band material,[5] showing good agreement with experiment within the limits of the approach. Nevertheless, as we will see in Sec. II, a shift of the conduction-band energies will be needed to correct the underestimation of the band gap given by DFT methods.

The real part of the dielectric tensor was obtained from the imaginary part by using the Kramers-Krönig relations. To get converged electronic properties and a frequency-dependent dielectric tensor, a 280 eV energy cutoff was used for the basis set and the following grids were needed to sample the Brillouin zone: $MgIn_2S_4$: $10\times10\times10$; $Mg_2TiIn_3S_8$ and $Mg_2VIn_3S_8$: $8\times8\times8$; $CdIn_2S_4$: $16\times16\times16$; $Cd_2TiIn_3S_8$ and $Cd_2VIn_3S_8$: $10\times10\times10$. All grids including the Γ point.

For both families, the pure semiconductors need more *k* points than their corresponding intermediate-band derivatives. This is because the dependence of the bottom conduction band, with the *k* points around Γ, is more pronounced for the pure compounds. Thus, we need more *k* points to accurately sample it (see Figs. 1, 2, 5, and 6 in Sec. II). For the three compounds with Mg, around 35 empty bands were needed to obtain convergence in the range of photon energies from 0 to 5 eV, whereas for the compounds with Cd we needed 45 empty bands.

III. RESULTS AND DISCUSSION

A. Structural properties

$MgIn_2S_4$ and $CdIn_2S_4$ crystallize in the cubic spinel structure (space group *Fd*-3*m*). This structure is characterized by a FCC sublattice of the sulfurs with Mg or Cd atoms occupying the tetrahedral sites, while In occupies the octahedral sites (this is the so-called *direct spinel* structure). In nature, however, partial situations can be found. Some cations can interchange their positions in the cell structure. In the limiting case, all of the Mg (or Cd) atoms occupy octahedral sites. Thus, half of the In atoms occupy the tetrahedral sites (this is called the *inverse spinel* structure). We can thus define the degree of inversion *x* as the number of Mg or Cd atoms at tetrahedral sites per chemical formula (0 for the inverse structure, 1 for the direct one, and values in between for partial situations).[14]

$MgIn_2S_4$ is assumed to have a degree of inversion of x=0.16 in nature (thus, almost inverse),[22,23] while the ac-

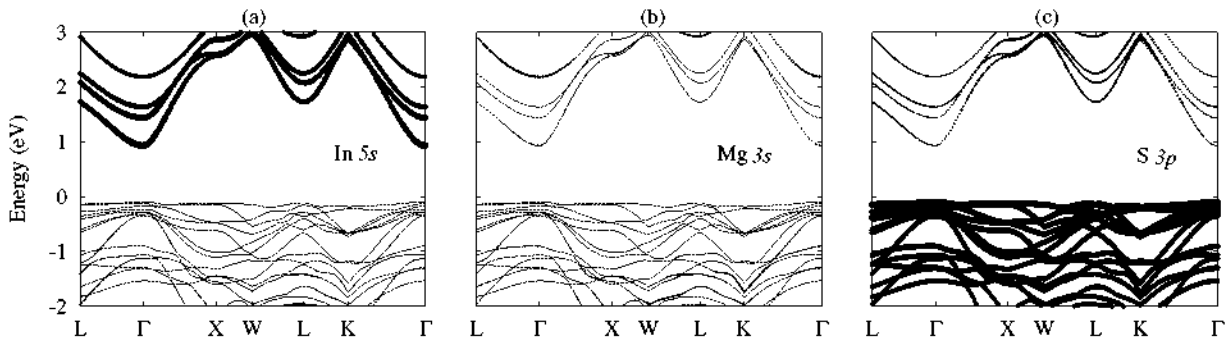

FIG. 2. (Color online) Projection of the band diagram of $MgIn_2S_4$, where the circles size is proportional to the orbital projections of the (a) In 5*s*, (b) Mg 3*s*, and (c) S 3*p* states divided by the number of atoms of each species. The contribution of other orbitals is comparatively negligible in this energy range. As a guide to the eye, the band diagram containing all the states is represented as a thin dashed line.

cepted value of x for $CdIn_2S_4$ is 0.80 (practically direct).[24] For the representation of these accepted values of the inversion, very large supercells would be needed. Therefore, we will study, for simplicity, the direct structure for $CdIn_2S_4$ and the inverse one for $MgIn_2S_4$, which are the closest to the experiments. By contrast, previous works only studied the direct structure for the Mg compound.[4]

Even for perfect direct spinels, there is always a distortion parameter that has to be taken into account. The *internal anion distortion parameter* (u) represents the distortion of the sulfur FCC sublattice, owing to the fact that each anion has three In and one Cd (or Mg) as nearest neighbors. Thus, the equilibrium position of the sulfurs is closer to one of the species. For our case, it is closer to Cd (or Mg).

In all cases, the transition metal (Ti or V) substitutes an In atom at octahedral sites, as it has been said that this coordination is normally more stable for these transition metals. The cell geometry, lattice parameters, and internal anion distortion u were determined by theoretical relaxation, by minimization of forces and total energy. In Tables I and II, we summarize the structural parameters obtained after this relaxation.

For pure $CdIn_2S_4$ direct spinel (see Table I), the relaxed lattice parameter is slightly overestimated with respect to the experimental one. However, the error is within an order of magnitude of usual GGA calculations.[27]

Once the substitution with the transition metal M has been made, a small tetragonal distortion appears due to the anisotropic environment of the octahedral sites.[15] The final structures have a lattice parameter c that is smaller by an amount on the order of 0.05 Å (see last two columns in Table I). The lattice parameters of both substituted alloys decrease with respect to that of the host semiconductor. This is due to the fact that Ti and V atoms are smaller than In and so the M-S distances are found to be shorter than those of In-S in the pure compound. The internal anion distortion remains practically equal to that of the parent semiconductor, which is in good agreement with experiment. Substitution with the transition metal generates two different environments for the S atoms and, thus, two values of u. For comparison with the host semiconductor, the u displayed in the table is that of sulfurs that retain the environment they had in the pure compound (i.e., three In and one Cd as neighbors).

In Table II we show the structural properties of $MgIn_2S_4$ and its intermediate-band derivatives. For the pure Mg semiconductor, as for the Cd one, relaxations lead to lattice parameters slightly above the experimental ones. However, these are still within the errors of typical GGA calculations. As the cell for this compound was constructed in an inverse spinel structure, the octahedral sites are anisotropically surrounded. This can be seen from In_{oct}-S and Mg-S bond lengths in Table II. This slightly lowers the symmetry of the cell from perfect cubic to tetragonal, as has been found for other spinels.[15,28] This distortion makes the lattice parameter c shorter than a and b. Additionally, in the inverse structure, there are different environments for the sulfurs and, thus, the

TABLE I. Lattice parameters a (in Å) and c/a, internal distortion u, and atomic distances (in Å) for $CdIn_2S_4$ and its derivatives. Comparisons with experiments, when available, are shown in brackets. In braces, the number of neighbors at each distance is shown.

	$CdIn_2S_4$	$Cd_2TiIn_3S_8$	$Cd_2VIn_3S_8$
a	11.014(10.797,[a]10.838–10.860)[b]	10.918	10.867
c/a	1	0.994	0.996
u	0.384(0.386)[a]	0.385	0.384
d(In-S)	2.65{6}(2.59)[a]	2.62{2}–2.67{4}	2.62{2}–2.66{4}
d(Cd-S)	2.56{4}(2.54)[a]	2.55{1}–2.56{3}	2.54{1}–2.56{3}
d(M-S)		2.51{6}	2.47{6}

[a]Experimental result of Hahn *et al.* (Ref. 25).
[b]Experimental result of Lee *et al.* (Ref. 26).

TABLE II. Lattice parameters a (in Å) and c/a, as well as atomic distances (in Å) for $MgIn_2S_4$ and its derivatives. Comparisons with experiments and other theoretical work, when available, are shown in brackets. In braces, the number of neighbors at each distance is shown.

	$MgIn_2S_4$	$Mg_2TiIn_3S_8$	$Mg_2VIn_3S_8$
a	10.869(10.50,[a]10.71)[b]	10.769	10.741
c/a	0.997	0.992	0.992
$d(In_{oct}\text{-}S)$	2.63{2}–2.66{4}(2.58)[c]	2.59{2}–2.66{4}	2.60{2}–2.66{4}
$d(In_{tet}\text{-}S)$	2.50{2}–2.54{2}(2.58)[c]	2.50{1}–2.51{1}–2.55{2}	2.49{1}–2.52{1}–2.55{2}
d(Mg-S)	2.59{4}–2.60{2}(2.48)[c]	2.53{2}–2.61{4}	2.53{2}–2.60{2}–2.62{2}
$d(M\text{-}S)$		2.49{2}–2.51{4}	2.45{2}–2.48{4}

[a]Other theoretical work (Ref. 14).
[b]Experimental work of Gastaldi *et al.* (Ref. 23).
[c]Experimental result of Hahn *et al.* (Ref. 25).

value of the internal anion distortion u is not unique.

As we can see, we have four different values for the In-S distance, owing to the different environments of indium and sulfur atoms. The average of this distance is in very good agreement with the experimental value reported by Hahn *et al.*[25] The Mg-S bond lengths are slightly overestimated (around 0.11 Å) with respect to the experiment. These differences may be due to the degree of inversion of the experimental samples: the value of 2.48 Å in Ref. 25 may have a contribution from a percentage of tetrahedral In, and the value of 2.58 can be also affected by the presence of octahedral Mg.

Substitution with the transition metal M implies that the lattice parameters decrease by around 0.1 Å, with respect to those of the host semiconductor. The M-S distances are also found to be shorter than those of In-S in the pure compound because of the sizes of Ti and V.

B. Electronic properties

1. Pure host semiconductors

For the pure semiconductors, the GGA band gaps were found to be 0.90 eV for inverse $MgIn_2S_4$ (it was previously obtained elsewhere[4] only for the direct spinel structure as 1.65 eV) and 1.05 eV for $CdIn_2S_4$. The first one was predicted as direct, in agreement with the work of Ruiz-Fuertes *et al.*[8] The gap of the Cd-compound was obtained as indirect, in agreement with predictions by other authors,[11–13] and we found the top of the valence band along the X-W direction (see Fig. 1). The difference between the indirect and direct (1.16 eV) band gaps of $CdIn_2S_4$ may be relevant for the study of optical properties, as indirect transitions will not be taken into account. Nevertheless, the contribution of indirect transitions is expected to be much lower than that of the direct ones. The fact that the difference between the direct and indirect band gaps is so small (0.11 eV in our calculation) may be responsible for the controversy between different authors.[8,10–13] These band-gap results should be compared to experimental values: 2.1–2.28 eV for $MgIn_2S_4$ and 2.0–2.2 eV for $CdIn_2S_4$. In any case, our GGA gaps are underestimated, as expected from a DFT approach (see, e.g., Ref. 29 and references therein). This will make it necessary to shift the excited states, in order to obtain appropriate optical spectra.

Owing to a lack of results for the band structures of Mg (Ref. 9) and Cd (Refs. 11, 30, and 31) spinels, a deeper study into the character of the bands and the origin of the gap is valuable. For $CdIn_2S_4$, we find that the topmost valence band (see Fig. 1) has mainly S $3p$ character, and the lowest conduction band is formed by mostly In $5s$ and Cd $5s$ states. This indicates that the value of the band gap is determined mainly by the In-Cd interaction, because the dispersion of

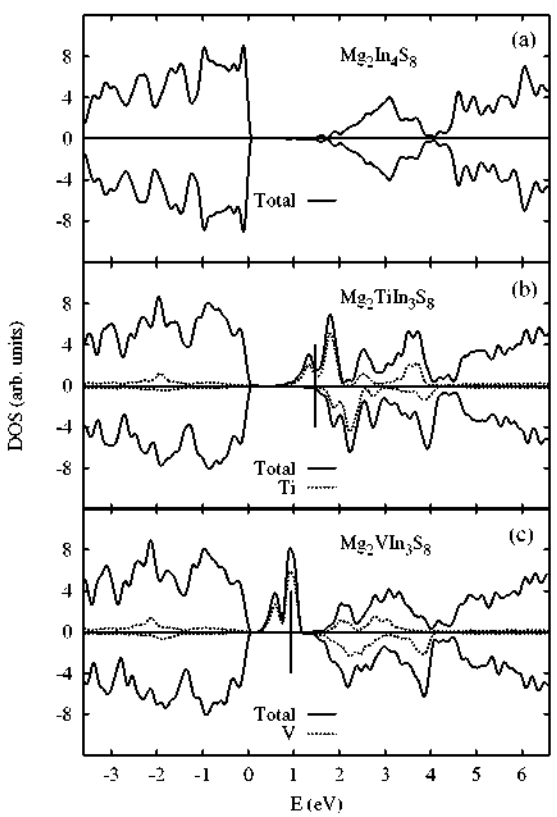

FIG. 3. (Color online) Total (solid line) and transition-metal projected (dotted line) densities of states (DOS) of the (a) $MgIn_2S_4$ semiconductor, (b) Ti-substituted alloy and (c) V-substituted compound (up and down spins), aligned at the valence-band maximum. Black vertical lines indicate the Fermi energy.

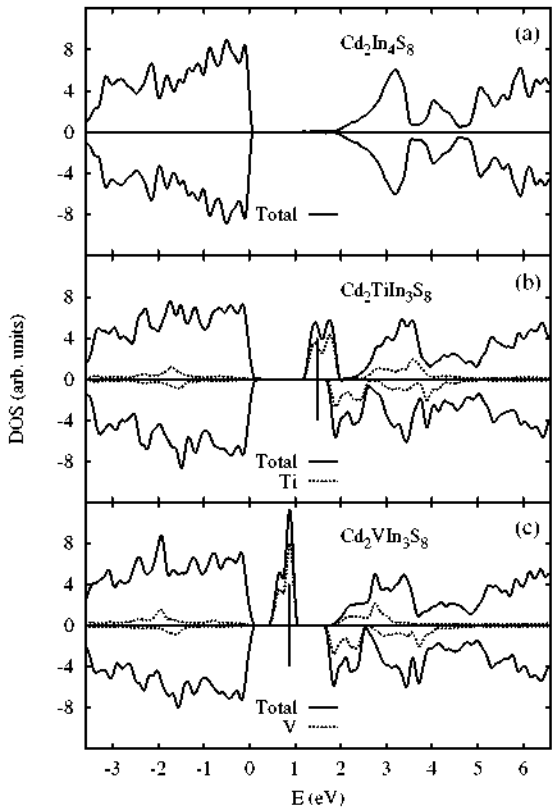

FIG. 4. (Color online) The same as Fig. 3, but for the $CdIn_2S_4$ derivatives.

the bottom conduction band depends on this interaction. This is in agreement with Ref. 8, where conclusions have been extrapolated from the spinel $CdIn_2O_4$. However, these results cannot be extrapolated for the Mg-spinel because, as can be seen in Fig. 2, the top valence band still has mainly S $3p$ character, but there is almost no contribution from the Mg states to the bottom of the conduction band, which is formed mainly by In.

2. Intermediate-band materials

Transition metals Ti and V were chosen as the best substituent candidates because, in an octahedral environment, their $3d$ t_{2g}-type states can form the partially filled intermediate band.

Figures 3 and 4 show the resulting density of states before and after the insertion of the transition metal. The projection on the transition-metal states is also displayed. The electronic structure of the substituted alloys presents a spin-polarized partially filled intermediate band formed by the majority-spin t_{2g} states, whereas the e_g and minority-spin d states appear highly hybridized with the conduction band. Figures 3(a) and 4(a) represent the electronic structure of the two parent semiconductors for comparison with their derivatives.

Figures 3(b) and 4(b) show the effect of Ti substitution. In both cases, due to the similar electronic structure of the two parent semiconductors, the resulting intermediate band is similar in width and position. The main difference is due to the fact that the $MgIn_2S_4$ pure semiconductor has a slightly

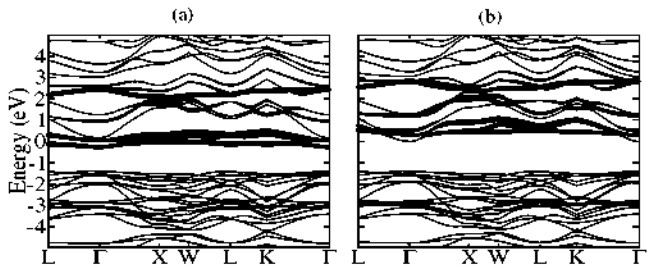

FIG. 5. (Color online) (a) Spin-up and (b) spin-down band diagrams of $Cd_2TiIn_3S_8$. The size of the red circles is proportional to the orbital projection of the Ti d states.

smaller band gap than $CdIn_2S_4$. Thus, the intermediate band in the case of $Mg_2TiIn_3S_8$, slightly overlaps with the conduction band.

If we now focus on the compounds with vanadium [see Figs. 3(c) and 4(c)], they also share similar features. However, in this case the main difference is that, for $Cd_2VIn_3S_8$, the IB is narrower than that of $Mg_2VIn_3S_8$. This effect is due not only to the differences between Cd and Mg, but also to the fact that the first one is a direct spinel and the second one is an inverse spinel. This means that, in the second case, the octahedral environment of the transition metal is distorted in one direction (see the bond lengths in Table II) and, thus, one of the three t_{2g} bands is separated from the others, making the intermediate band appear thicker.

To see the effect of the concentration of transition metal on the intermediate-band formation, we performed calculations at different dilution levels. Cells of 14, 28, and 56 atoms were studied (1/4, 1/8, and 1/16 replacement of In by the transition metal, respectively). We found that the intermediate band appears at the same position and with similar widths and features for the different concentrations.

To better understand the formation of the IB, band diagrams of the derivatives of $CdIn_2S_4$ and a projection of the transition-metal states were obtained, as shown in Figs. 5 and 6 (the features are very similar for the derivatives of $MgIn_2S_4$). From these figures, it can be more precisely seen how the spin-up t_{2g} states form the intermediate band inside the gap of the host semiconductor, which is isolated from the valence and conduction bands. In addition, it can be seen how, as mentioned above, the e_g states hybridize with the conduction band.

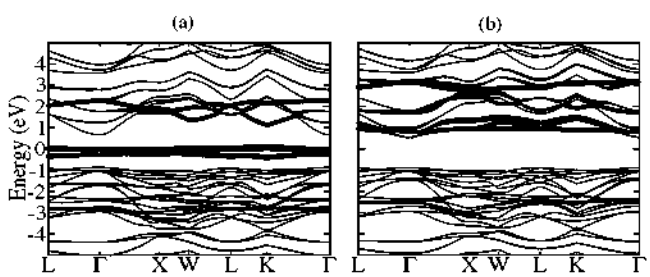

FIG. 6. (Color online) (a) Spin-up and (b) spin-down band diagrams of $Cd_2VIn_3S_8$. The size of the red circles is proportional to the orbital projection of the V d states.

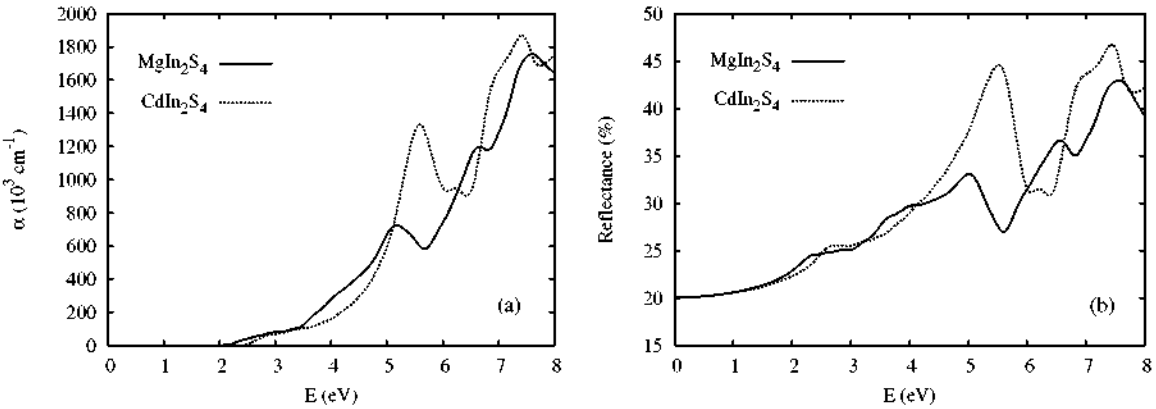

FIG. 7. (Color online) (a) Absorption coefficient and (b) reflectance of the two host semiconductors.

C. Optical properties

1. Pure host semiconductors

As we have already mentioned, it is well known that standard DFT significantly underestimates the band gap of semiconductors. A correction to the conduction band is thus necessary for the proper determination of excited states characteristics such as optical properties. There are several facts demonstrating that this, although simple, is a reasonable correction. The good agreement with experiment of the absorption coefficient of the IB material V-substituted In_2S_3, when a rigid shift is applied to the conduction eigenvalues[5] and previous exact exchange calculations for other IB materials,[32] show that the correction is appropriate. In addition, this shift between the intermediate and conduction bands has also been found by other authors to be the most reasonable in these cases.[2]

First of all, the absorption coefficient and reflectance of the host semiconductors were computed to be used as a reference for the substituted materials, and they are displayed in Fig. 7. The similar character of the bands for both semiconductors gives rise to similar optical properties.

These optical properties were compared with the few available experimental results in the literature.[6–8,13,33] There is a lack of a complete description of the optical properties of these compounds, as most of optical studies focus on the absorption edge and not on overall spectra in the visible range.

In the case of $CdIn_2S_4$, when a larger energy range has been studied in the literature,[33] results are highly dependent on the sample because of the very different qualities of the reflecting surface of the samples. This is one of the reasons why our reflectance spectrum is higher in intensity than those of the experiments. In spite of this fact, the main features of our calculations [peaks around 5.5 and 7.5 eV in Fig. 7(b)] agree in energy with those peaks found experimentally in Ref. 33.

For the Mg compound, one of the very few available experimental optical results is the refractive index.[22] The corrected-band-gap value agrees better with the experiment, within the typical precision of DFT, as can be seen in Table III.

TABLE III. Calculated and experimental refractive index n of the two spinel host semiconductors.

	n (GGA)	n (gap-corrected GGA)	n (experimental)
$MgIn_2S_4$	2.906	2.624	2.41[a]
$CdIn_2S_4$	2.893	2.625	

[a]Experimental result of Wakaki *et al.* (Ref. 22).

2. Intermediate-band materials

Let us first focus on the absorption coefficients obtained for the derivatives of $MgIn_2S_4$. Figures 8 and 9 show the absorption coefficients of Ti and V-substituted $MgIn_2S_4$, compared to that of the pure semiconductor. The solar spectrum is displayed as a background to show the enhancement in absorption due to the IB in the main part of the solar spectrum.

As the optical absorption properties are calculated as a sum over independent transitions, we can obtain the individual contribution of a given set of bands. To reveal the specific effect of the transition-metal band on the optical

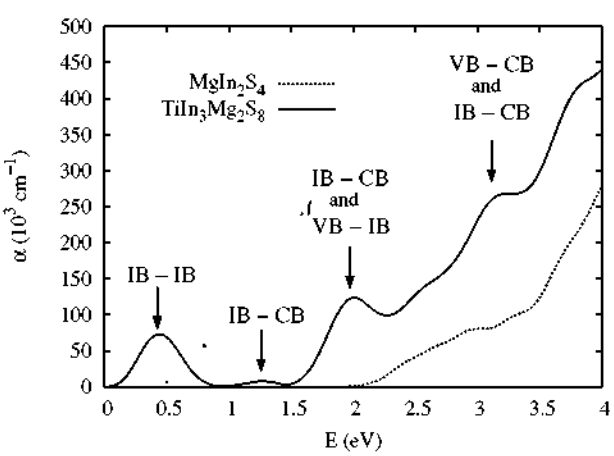

FIG. 8. (Color online) Absorption coefficient of the Ti-substituted $MgIn_2S_4$ intermediate-band compound, compared to that of the host semiconductor. Interpretation of the main peaks through the transitions involving the intermediate band. The AM1.5G solar spectrum in the background is shown as a reference.

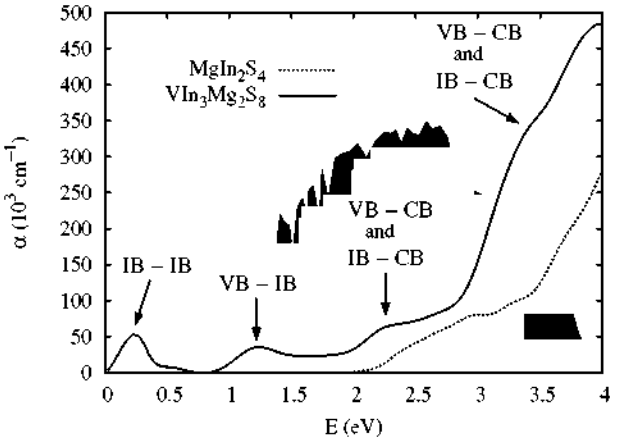

FIG. 9. (Color online) The same as Fig. 8, but for the V-substituted $MgIn_2S_4$ alloy.

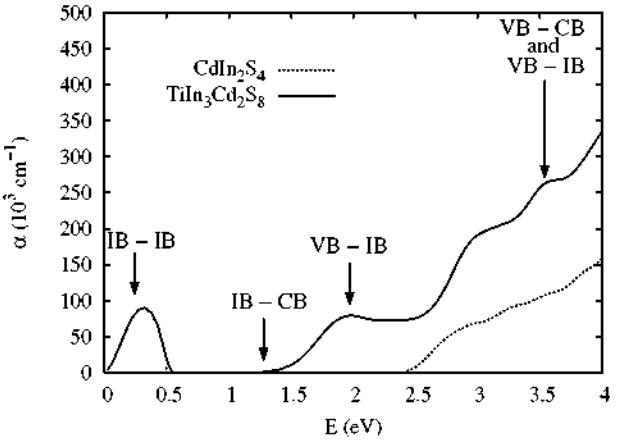

FIG. 10. (Color online) Absorption coefficient of the Ti-substituted $CdIn_2S_4$ intermediate-band compound compared to that of the host semiconductor. Interpretation of the main peaks through the transitions involving the intermediate band. The AM1.5G solar spectrum in the background is shown as a reference.

spectra, we have indicated on the figures the transitions that mainly contribute to each peak. For all intermediate-band materials, the first peak in the absorption is due to transitions between different states of the IB. These transitions contribute indirectly to the overall dynamic process of absorption,[34] but they are not used in the generation of photocurrent in the cell. This is because one requirement of the intermediate band is to be isolated from the contacts of the cell. Thus, the creation of electron-hole pairs in the IB will not directly increase the photocurrent of the device.

Fot Ti as the substituent, the two transitions involving the IB contribute mainly to the peak around 2 eV (see Fig. 8). This is the main effect; however, there is a small contribution from these transitions across the whole solar spectrum. The principal difference with the case of vanadium as substituent (see Fig. 9) is that, in this latter case, the two additional transitions, from valence band (VB) to IB and from IB to conduction band (CB), contribute at different energies. This situation is better, in principle, as the aim of the intermediate band is to cover with these additional peaks the maximum range of energies of solar emission. In Fig. 9, the first peak around 1.2 eV is due to transitions between the VB and IB, while the second peak around 2.2 eV is principally due to transitions between the IB and CB (apart from the contribution between valence and conduction bands, which was already present in the pure semiconductor). The position of the intermediate band inside the band gap becomes an important factor to be taken into account, as it will determine the onsets of contributions toward the total absorption coefficient.

In analogy with the interpretation for the $MgIn_2S_4$ derivatives, Figs. 10 and 11 show analysis of the absorption coefficients of Ti and V-substituted $CdIn_2S_4$. Again, due to the similar electronic properties between the compounds with Mg and those with Cd, the optical properties present a similar behavior. In the case of Ti in Fig. 10, the main peak at 2 eV is formed by transitions between the VB and IB, even though the onset at 1.4 eV is determined by transitions between the IB and CB. Features of the last two peaks around 3 and 3.5 eV are determined principally by transitions from the VB to CB but with small contributions from the other two possible transitions (VB to IB and, to a lesser extent, IB to CB). V-substituted $CdIn_2S_4$ is analyzed in Fig. 11, where the main contribution of the intermediate band is the peak around 1.2 eV. This is not in the region of higher solar emission, compared to the Ti peak, but at least there is some absorption below 1 eV that was missing in the Ti alloy. Therefore, for Ti, we have an intermediate band that does not allow absorption below 1 eV but favors the absorption of the main range of the solar spectrum. In contrast, the IB of the V alloy allows the absorption of photons of all energies, but in the main part of the spectrum the absorption is weak.

To assess which of these two situations is better for absorption, we analyzed the factor given by the integral of the product of $\alpha(\omega)$ and the solar spectrum $I(\omega)$: $F=\int_0^\infty \alpha(\omega)\times I(\omega)d\omega$. This factor can be interpreted as an efficiency of the absorption of the sun's light, which is an additional parameter that is taken into account to determine the most suitable intermediate-band absorber.

The values of this parameter are shown in Table IV. The fact that this factor is bigger for the two compounds with Ti can be attributed to the wider intermediate bands, compared

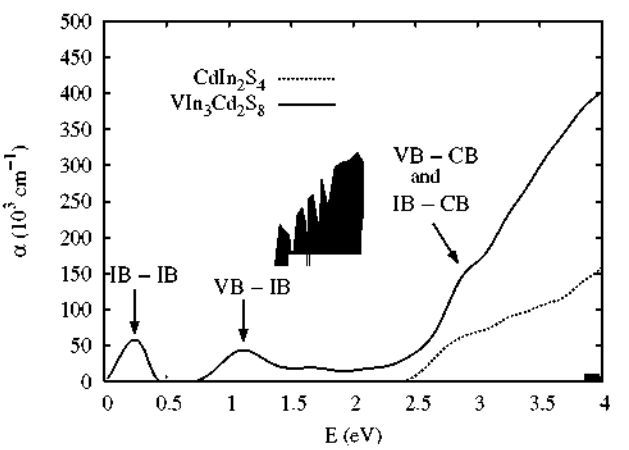

FIG. 11. (Color online) The same as Fig. 10, but for the V-substituted $CdIn_2S_4$ alloy.

TABLE IV. Area of the product of $\alpha(\omega)$ and the solar spectrum $I(\omega)$ (in arb. units).

$CdIn_2S_4$	$Cd_2TiIn_3S_8$	$Cd_2VIn_3S_8$
783	2883	2359
$MgIn_2S_4$	$Mg_2TiIn_3S_8$	$Mg_2VIn_3S_8$
1155	3855	2879

to those of the V compounds (see Figs. 3 and 4) and to the better position of the IB inside the gap. It should also be noticed that the Mg-based compounds (including the semiconductor) have bigger factors than the Cd-based compounds. This is also due to the wider intermediate band, but mainly because of the better position of the absorption edge of the host semiconductor. From these numbers we can conclude that the best absorber would be $Mg_2TiIn_3S_8$. Nevertheless, other factors should be taken into account to make the final decision: for example that the two transitions involving the IB occur at approximately the same rate, or the recombination processes and electron-hole mobilities.

3. Transmittance

The transmittance of the different compounds can be derived from their absorption coefficient and reflectance. It has been studied here as a function of the thickness of the sample w to reveal and highlight the importance of this parameter. The thicknesses have been chosen in the range of typical widths of thin-film absorbers in solar cells.

Figures 12 and 13 display the transmittance of the transition-metal alloys derived from $MgIn_2S_4$ and $CdIn_2S_4$, respectively. We can see that thicknesses below approximately 2 μm have a large influence on the absorption and that part of the effect of the IB is lost.

In view of these results, the optimization of w should be taken into account by finding a compromise between the

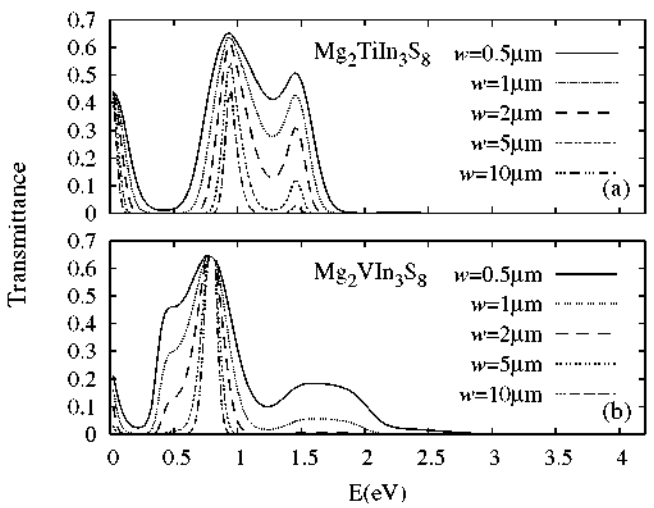

FIG. 12. (Color online) Transmittance of the intermediate-band derivatives of $MgIn_2S_4$ as a function of the width of the sample w.

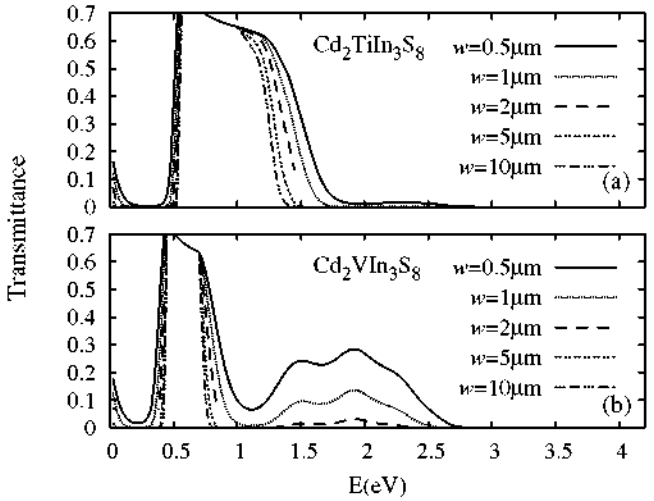

FIG. 13. (Color online) The same as Fig. 12, but for the derivatives of $CdIn_2S_4$.

absorption and the negative effects of a sample that is too thick. On the one hand, the thicker the sample, the higher the absorptivity. On the other hand, a thinner absorber will prevent some recombination effects and reduce the cost of final devices. It is thus important to combine our transmittance results with experimental studies of the recombination, to find the optimum width for absorbers in this kind of solar cells. However, as no experimental results are yet available for these intermediate-band alloys, this study is a first step in the estimation of this ideal width.

IV. SUMMARY AND CONCLUSIONS

We have analyzed and compared two thiospinel-type semiconductors: $MgIn_2S_4$, with an inverse spinel structure, and $CdIn_2S_4$, with a direct structure. The electronic properties of these semiconductors were obtained, and, to better understand the origin of their band gap, an analysis of the band character was carried out. The optical properties of these compounds have been discussed and we find good agreement with the few experimental results, measured in the optical frequency range of interest, found in the literature.

Once the parent semiconductors were well understood, we proceeded to the substitution of In atoms by transition metals such as V and Ti. These substituents were chosen among other transition metals because their t_{2g} states form an isolated spin-polarized partially filled band inside the band gap of the host semiconductor. The effect of the structural degree of inversion on the intermediate-band formation has been assessed, by studying a direct and an inverse-structure compounds and comparing them.

Full relaxation of the atomic structures shows that, in the case of the inverse structures, some symmetries are lost, and thus the cell has a small tetragonal distortion. This affects the octahedral environment of the transition metals as well, which is contracted in one of the directions, making one of the t_{2g} states slightly separated from the others. This gives rise to a thicker intermediate band. For the direct spinel structures, after the substitution with transition metals, the

symmetry is also lowered from perfectly cubic to tetragonal due to the nonisotropic environment of the transition metals. However, values of the internal anion distortion parameter are retained with respect to that of the host semiconductor. For all the substituted alloys, the lattice parameter is reduced by about 0.1 Å with respect to that of the pure semiconductor, due to the fact that Ti and V atoms are smaller than In.

Due to the suitability of the electronic structure of these materials for photovoltaic applications, their optical properties were discussed. Absorption coefficients show additional peaks due to the transition-metal band, appearing at energies in the range of higher solar emission, which was a region of forbidden absorption for the pure semiconductors. From the absorption coefficient and the reflectance, the transmittance T of the compounds can be determined as a function of the width of the absorber. We have thus obtained T for several widths on the order of magnitude of typical thin-film absorbers in solar cells. By means of these transmittances, we have gone a step further in trying to determine the optimum width of these materials, which should be combined with experimental recombination studies as a final step.

In summary, we have considered interband and direct transitions for the calculation of optical properties, to predict the best transition-metal substituent in two thiospinel semiconductors in the quest for an efficient photovoltaic material. All the compounds shown here fulfill the desired requirements for an efficient intermediate-band absorber, both from electronic and optical analyses. Experimental preparations of these materials have been initiated, and we believe that this work will help in the interpretation and understanding of future experiments.

ACKNOWLEDGMENTS

This work was supported by the Ministerio de Ciencia e Innovación through the projects Consolider Ingenio 2010 GENESIS-FV (Grant No. CSD2006-04) and FOTOMAT (Grant No. MAT2009-14625-C03-01) and a FPU grant (I.A.). We acknowledge the Comunidad de Madrid for the project NUMANCIA (Grant No. S-05050/ENE/0310) and the grant of K.S. The computer resources provided by the Madrid Supercomputing Center (CeSViMa) are also acknowledged.

[1] A. Luque and A. Martí, Phys. Rev. Lett. **78**, 5014 (1997).
[2] P. Olsson, C. Domain, and J.-F. Guillemoles, Phys. Rev. Lett. **102**, 227204 (2009).
[3] P. Palacios, K. Sánchez, J. C. Conesa, and P. Wahnón, Phys. Status Solidi A **203**, 1395 (2006); P. Palacios, K. Sánchez, J. C. Conesa, J. J. Fernández, and P. Wahnón, Thin Solid Films **515**, 6280 (2007); P. Palacios, K. Sánchez, P. Wahnón, and J. C. Conesa, ASME J. Sol. Energy Eng. **129**, 314 (2007).
[4] P. Palacios, I. Aguilera, K. Sánchez, J. C. Conesa, and P. Wahnón, Phys. Rev. Lett. **101**, 046403 (2008).
[5] R. Lucena, I. Aguilera, P. Palacios, P. Wahnón, and J. C. Conesa, Chem. Mater. **20**, 5125 (2008).
[6] P. M. Sirimanne, N. Sonoyama, and T. Sakata, J. Solid State Chem. **154**, 476 (2000).
[7] M. Wakaki, O. Shintani, T. Ogawa, and T. Arai, Jpn. J. Appl. Phys. **19**, Suppl. 19-3, 255 (1980).
[8] J. Ruiz-Fuertes, D. Errandonea, F. J. Manjón, D. Martínez-García, A. Segura, V. V. Ursaki, and I. M. Tiginyanu, J. Appl. Phys. **103**, 063710 (2008).
[9] S. Katsuki, Solid State Commun. **39**, 767 (1981).
[10] Y. Li, R. Dillert, and D. Bahnemann, Thin Solid Films **516**, 4988 (2008).
[11] F. Meloni and G. Mula, Phys. Rev. B **2**, 392 (1970).
[12] K. Y. Rajpure, V. L. Mathe, and C. H. Bhosale, Bull. Mater. Sci. **22**, 927 (1999).
[13] H. Nakanishi, S. Endo, and T. Irie, J. Phys. (Paris), Colloq. **36**, C3-163 (1975).
[14] M. Marinelli, S. Baroni, and F. Meloni, Phys. Rev. B **38**, 8258 (1988).
[15] A. Seko, K. Yuge, F. Oba, A. Kuwabara, and I. Tanaka, Phys. Rev. B **73**, 184117 (2006).
[16] J. P. Perdew, J. A. Chevary, S. H. Vosko, K. A. Jackson, M. R. Pederson, D. J. Singh, and C. Fiolhais, Phys. Rev. B **46**, 6671 (1992).
[17] G. Kresse and J. Hafner, Phys. Rev. B **47**, 558 (1993); G. Kresse and J. Furthmüller, *ibid.* **54**, 11169 (1996).
[18] G. Kresse and D. Joubert, Phys. Rev. B **59**, 1758 (1999).
[19] P. E. Blöchl, Phys. Rev. B **50**, 17953 (1994).
[20] M. Gajdoš, K. Hummer, G. Kresse, J. Furthmüller, and F. Bechstedt, Phys. Rev. B **73**, 045112 (2006).
[21] J. Furthmüller, http://www.freeware.vasp.de/VASP/optics/.
[22] M. Wakaki, O. Shintani, T. Ogawa, and T. Arai, Jpn. J. Appl. Phys. **21**, 958 (1982).
[23] L. Gastaldi and A. Lapiccirella, J. Solid State Chem. **30**, 223 (1979).
[24] V. V. Ursaki, F. J. Manjón, I. M. Tiginyanu, and V. E. Tezlevan, J. Phys.: Condens. Matter **14**, 6801 (2002).
[25] H. Hahn, W. Klingler, and Z. Anorg, Z. Anorg. Allg. Chem. **263**, 177 (1950).
[26] S.-J. Lee, J.-E. Kim, and H.-Y. Park, J. Mater. Res. **18**, 733 (2003).
[27] A. E. Mattsson, R. Armiento, J. Paier, G. Kresse, J. M. Wills, and T. R. Mattsson, J. Chem. Phys. **128**, 084714 (2008).
[28] P. G. Radaelli, New J. Phys. **7**, 53 (2005).
[29] O. A. von Lilienfeld and P. A. Schultz, Phys. Rev. B **77**, 115202 (2008).
[30] W. Rehwald, Phys. Rev. **155**, 861 (1967).
[31] A. A. Lavrent'ev, N. Y. Safontseva, V. A. Dubeiko, B. V. Gabrel'yan, and I. Y. Nikiforov, Phys. Solid State **42**, 2047 (2000).
[32] J. J. Fernández, C. Tablero, and P. Wahnón, Comput. Mater. Sci. **28**, 274 (2003).
[33] M. Turowski, A. Kisiel, and J. Giriat, J. Phys. C **17**, L661 (1984).
[34] M. Levy and C. Honsberg, J. Appl. Phys. **104**, 113103 (2008).